Optimum Supersonic Wings with Subsonic Leading Edges

H. J. Bos*
Delft University of Technology, Delft, the Netherlands

Results from linearized wing theory are employed to study the planform optimization for supersonic wings with subsonic leading edges. Momentum flux theory in a characteristic control surface is used to minimize the drag of a supersonic nonslender delta-like wing with subsonic leading edges and a supersonic trailing edge producing a given lift. In this paper a method is presented to construct the so-called Hayes-cuts of the optimum lift distribution. The method is applied to wings with two types of trailing edges. The results indicate that in general the optimum lift distribution for minimum total drag differs from the elliptical distribution obtained to produce minimum wave drag. Since the shape of the subsonic leading edges need not be specified in the present method, nonuniqueness of the optimum planform seems to exist.

Nomenclature

a = radius of the circular contour C_1^*
a_0 = speed of sound in the undisturbed flow
b = semispan of the wing
c = chord of the wing
C_1 = intersection curve of the forward-facing and rearward-facing parts of the control surface
C_1^* = projection of the intersection curve C_1 on a plane normal to the x axis
C_2^* = projection of the wing on a plane normal to the x axis
D = drag force
f = transformed semispan $= 2b/[1+(b/a)^2]$
$f(y,z)$ = function describing the control surface
$g(y,z)$ = function describing a two-parameter family of planes
k $= \sqrt{1+(\beta^4-1)n_x^2}$
$\ell(y/b)$ = spanwise lift distribution
$\ell(x_0,\theta)$ = cross-load distribution
L = lift force
M_0 = Mach number of the undisturbed flow
n = degree of homogeneity of the flow
$\tilde{n}$ = unit normal vector
p = complex coordinate $= y+iz$
$\tilde{p}$ = complex coordinate in transformed plan $= u+iv = 2p/[1+(p/a)^2]$
S_c = control surface
S_p = projection of the control surface on a plane normal to the x axis
x,y,z = dimensional space coordinates
β $= \sqrt{M_0^2-1}$
λ = Lagrange multiplier
$\tilde{\nu}$ = unit conormal vector $= k\{-\beta^2 n_x, n_y, n_z\}$
$\varphi(x,y,z)$ = disturbance velocity potential
$\Phi_f(y,z)$ = velocity potential on the control surface $= \varphi\{x=f(y,z),y,z\}$
$\Phi_g(y,z)$ = velocity potential on the surface given by $\{x=g(y,z)\} = \varphi\{x=g(y,z),y,z\}$

Received May 3, 1985; revision received Sept. 30, 1985.

*Department of Aerospace Engineering.

Introduction

IN this paper, the minimization of the drag for a wing of zero thickness and given lift is analyzed using linearized supersonic wing theory. In particular, the optimum planform shape within a limited class of delta-like wings with subsonic leading edges is considered.

It is assumed that the homogeneous atmosphere in which the wing moves is an ideal gas with constant specific heats. Effects of viscosity, heat conduction (or other forms of heat supply), and gravity are ignored. In that case, the isentropic relation or Poisson's law applies. It follows then also from the Euler equations that Kelvin's theorem on the conservation of circulation applies. It is further assumed that the wing has no thickness, and that the plane of the wing makes a small angle with the velocity vector. This justifies the assumption that the wing produces only small perturbations in the flow.

It is convenient to formulate the problem in a reference system at rest with respect to the wing. Since the discussion will be limited to steady cases, this yields the problem of a thin wing placed at a small angle of attack in a uniform flow of speed U_0. If a_0 denotes the speed of sound in the uniform stream, it will be assumed that the velocity everywhere exceeds the value a_0 and so is supersonic throughout.

Since Kelvin's theorem applies, the vorticity in the flow is confined within a thin layer behind the wing: the wake. Hence, a disturbance velocity potential $\varphi(x,y,z)$ is introduced and, since the disturbance velocities generated by the wing are small compared with the undisturbed flow velocity U_0, the equations of motion are linearized. It is found that the disturbance velocity potential satisfies the wave equation in x,y,z coordinates (see Fig. 1).

$$\beta^2\varphi_{xx}-\varphi_{yy}-\varphi_{zz}=0 \tag{1}$$

Direct and Inverse Minimization Method

On the subject of drag minimization for a wing of zero thickness and a given lift, an extensive literature is available. The literature can be divided roughly into two parts, corresponding to the "close" and the "distant" viewpoints.

In one part the minimization problem is approached from a close viewpoint. On a given planform a series of camber distributions and the corresponding pressure distributions are combined in a proper way to obtain minimum drag. In accordance with the terminology of the calculus of variations, this method is called a "direct optimization" method. It is observed that this method has some limitations since both the planform and the minimizing sequence of camber distributions on the planform are restricted to the class for which the corresponding pressure distributions are known. Typical examples

of the direct method are due to D. Cohen,[1] S. H. Tsien,[2] and M. Fenain and D. Vallée.[3]

A less restricted approach can be made from a distant viewpoint. One of the equations of motion, the momentum equation, states that in the flow the stress tensor is balanced by the momentum flux tensor. Upon integration of this equation over a flow volume enclosing the wing and bounded by a so-called "control surface," it is found that the aerodynamic force acting on the wing is balanced by the sum of the pressure force on the control surface and the momentum flux through the control surface. Hence, the lift and the drag of the wing can be evaluated by integration of the corresponding components of the pressure force and the momentum flux through the surface control with the choice of the control surface still being free. The minimization of the drag for fixed lift then is formulated as a variational problem for the quantities at the control surface, and the solution is translated to conditions for the lift distribution on the wing. This second optimization method, starting from the distant viewpoint and yielding conditions for the lift distribution over the wing will, owing to these properties and in contrast with the direct optimization method, be called an inverse optimization method.

To the second optimization method belong the well-known work of R.T. Jones[4-7] and work of G.N. Ward,[8] M.K. Kogan,[9] Yu.L. Zhilin,[10] and M.A. Heaslet and F.B. Fuller.[11] In these papers the momentum flux method is applied on a control surface composed of two characteristic surfaces forming the separation between the disturbed and the undisturbed region in the direct and the reversed flow, respectively. Because of this special choice for the control surface, the relatively simple condition to be satisfied by the velocity potential $\varphi(x,y,z)$ in the control surface [given by the double valued function $x=f(y,z)$] in order to obtain minimum drag is

$$\Phi_{f_{yy}}+\Phi_{f_{zz}}=0 \tag{2}$$

In this paper, it is demonstrated that the momentum flux method may also be applied to delta-like wings with *subsonic* leading edges. This is illustrated with two examples, a wing with sonic trailing edges of the boattail type and a wing with a straight trailing edge perpendicular to the oncoming flow direction.

Application of Momentum Flux Method in a Characteristic Control Surface

The drag force D on the wing balances the sum of the impulse flux in x direction through the control surface and the x component of the pressure force on the control surface. Within linear theory, and with the special choice of the control surface indicated above and defined by $x=f(y,z)$ (Fig. 2), for D the following bilinear expression is found[9]:

$$D=\frac{\rho_0}{2}\int_{S_p}\int\{\Phi_{f_y}^2+\Phi_{f_z}^2\}\mathrm{d}S_p \tag{3}$$

In the same way, one finds for the lift

$$L=-\rho_0 U_0\int_{S_p}\int\Phi_{f_z}\mathrm{d}S_p \tag{4}$$

Minimum drag for given lift is obtained if (cf. Refs. 8 and 12)

$$\Phi_{f_{yy}}+\Phi_{f_{zz}}=0, \qquad \text{in } S_p \tag{5}$$

with the boundary conditions

$$\Phi_f=0, \qquad \text{at } C_1^*$$

$$\Phi_{f_z}=\text{const}=-\lambda U_0, \quad \text{at } C_2^* \tag{6}$$

If $\Phi_f(y,z)$ satisfies Laplace's equation (5) with the boundary conditions (6) one finds for D:

$$D=\frac{\lambda}{2}L \tag{7}$$

The solution of the boundary value problem [Eqs. (5) and (6)] clearly depends on the form of the curve C_1^* and, hence, on the supersonic parts of the edge of the planform. For delta-like planforms with subsonic leading edges, the solution is influenced only by the form of the trailing edge.

Sonic Trailing Edge

Consider a wing with sonic trailing edge of boattail type. (see Fig. 3).

The curve C_1^* is a circle, and upon conformal transformation an exact solution[12] for the boundary value problem in the transformed plane is obtained by inversion of a singular integral equation for the potential distribution at C_2^*:

$$\Phi_f^*(u,v)=Re\left[\lambda U_0\left\{\frac{2}{\pi}\sqrt{f^2-\tilde{p}^2}\left\{K\left(\frac{f}{a}\right)+\frac{a^2-\tilde{p}^2}{\tilde{p}^2}\Pi\left\{\left(\frac{f}{\tilde{p}}\right)^2,\frac{f}{a}\right\}\right\}+\frac{ia^2}{\tilde{p}}\right\}\right] \tag{8}$$

In Eq. (8) the functions $K(t)$ and $\Pi(\alpha^2,t)$ are complete elliptic integrals of the first and third kind, respectively. Once the solution is known, the parameter λ is determined by substitution of Eq. (8) in the expression for the lift, Eq. (4), yielding

$$\lambda=\frac{\pi}{4\rho_0 U_0^2 a^2}\times\frac{L}{\{\pi/2\}^2-\{E(f/a)\}^2-\{(a^2-f^2)/f^2\}\{K(f/a)-E(f/a)\}^2} \tag{9}$$

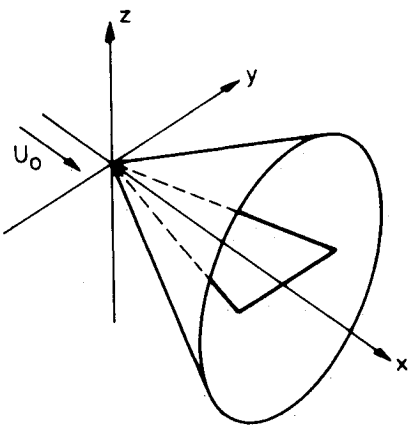

Fig. 1 Coordinate system and flow configuration.

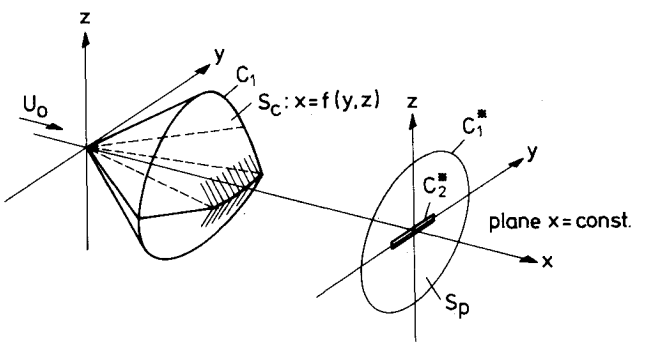

Fig. 2 Control surface and its projection.

The expression for λ[Eq. (9)] and Eq. (7) determine the lower bound of the drag. Figure 4 shows the gain that may be obtained with respect to the drag of a flat plate wing with straight leading edges as a function of the parameter $\bar{k}$ defined by

$$\bar{k}=\beta\frac{b}{s}=\beta\bar{m}=\frac{(b/a)}{2-(b/a)} \tag{10}$$

where $\bar{m}=b/s$ is the mean inclination of the leading edge.

The other two curves in Fig. 4 compare the drag of the flat plate wing with the drag of a wing with optimum camber and twist described by a homogeneous polynomial of degree n on the same planform and generating the same lift.

In addition to an overall property like the drag value, the optimum spanwise lift distribution is also obtained from the combination of Eqs. (9) and (8). In Fig. 5 the optimum spanwise lift distribution is plotted for various values of $\bar{k}$.

Straight Trailing Edge

For a wing with a straight trailing edge perpendicular to the oncoming flow direction, the curve C_1^* consists of two parabolic and two elliptical sections. In that case an exact solution is difficult to find, but an approximate solution can simply be constructed.

First, the curve C_2^* is transformed into a circle by means of a Joukowsky transformation and, hence, the region between the curves C_1^* and C_2^* in the y,z plane is mapped onto an annular region in the w plane (cf. Fig. 6).

In the w plane the solution is written as a Laurent series,

$$\Phi_f=Re\sum_{n=1}^{\infty}\left\{\frac{A_n}{w^n}+B_n w^n\right\} \tag{11}$$

Applying the boundary conditions [Eq. (6)] at C_2^* and taking the symmetry properties into account, the solution [Eq. (11)] may be rewritten as

$$\Phi_f(r,\varphi)=\sum_{p=0}^{\infty}\bar{A}_{2p+1}\{(1/r^{2p+1})+r^{2p+1}\}\sin(2p+1)\,\varphi$$
$$-\lambda U_0 br\sin\varphi \tag{12}$$

where the boundary conditions at C_1^* still have to be satisfied. If the curve C_1^* is given by $r=r_{c_1}(\varphi)$, the boundary condition at C_1^* determines the coefficients $\bar{A}_{2p+1}$.

A simple integration shows the lift to be

$$L=\pi\rho_0 U_0^2 b^2\lambda[2\bar{A}_1-1] \tag{13}$$

The parameter λ is found from Eq. (13), and the lower bound of the drag is determined again. Figure 7 shows the gain that may be obtained with respect to a flat plate wing with straight leading edges as a function of the parameter $\bar{k}$ [(Eq. (10)]. Figure 7 also shows the improvements in the delta wing planform obtained by application of an optimum combination of homogeneous flow solutions of degree n. Moreover, the figure shows a curve indicating the lower bound of the drag obtained electrical analogy.[13]

For this type of wing planform, the optimum spanwise lift distribution is plotted for various values of $\bar{k}$ (see. Fig. 8).

Generation of Cross-Load Distributions

Once the optimum potential distribution $\Phi_f(y,z)$ is known, the potential distribution has to be translated into a lift distribution on the plane of the wing. In this section a method indicated by Heaslet and Fuller[11] is extended and applied to optimum wings with subsonic leading edges. Interpreting the Prandtl-Glauert equation (1) as the divergence of a vector, upon integration of this equation over a volume V with a boundary S, one finds

$$\int_S\int\frac{1}{k}\frac{\partial\varphi}{\partial\nu}dS=0 \tag{14}$$

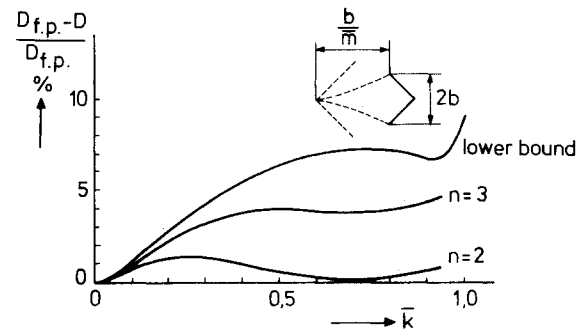

Fig. 4 Variation of drag reduction with slenderness for a wing planform with sonic trailing edge.

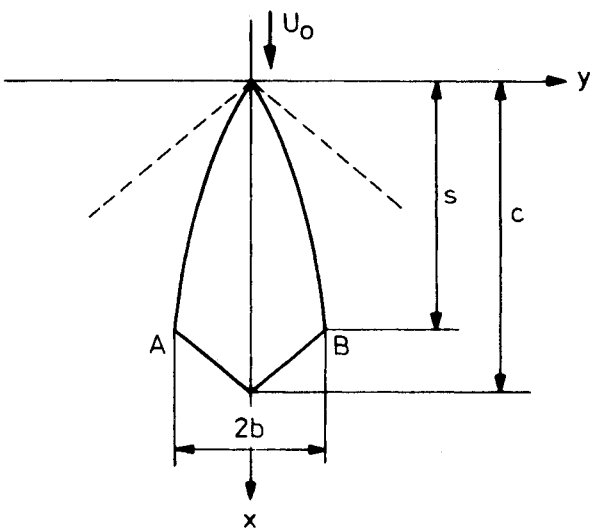

Fig. 3 Wing planform with sonic trailing edge.

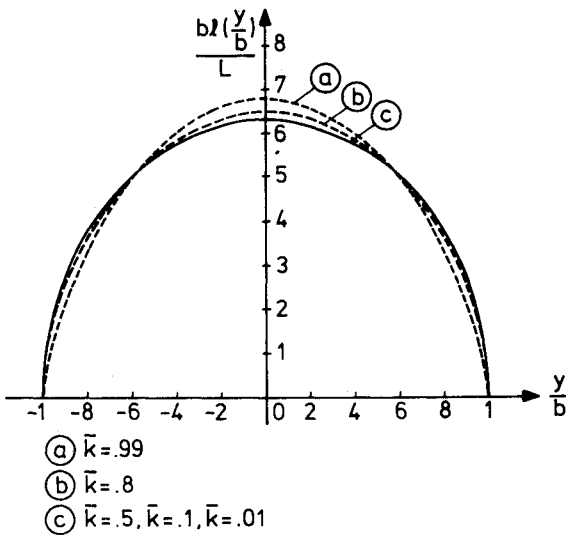

Fig. 5 Influence of slenderness on the optimum spanwise lift distribution for a wing planform with sonic trailing edge.

The integral theorem (14) is applied to a closed volume V_1 bounded by a surface S_1 composed of four parts (Fig. 9): S_M is the downstream Mach cone with vertex at the apex of the wing; S_F the envelope of the upstream facing characteristic cones with vertices on the trailing edge written as $x=f(y,z)$, S_w the surface of the wing, and S_g a two-parameter family of planes at fixed angle $a\tan 1/\beta$ with the x axis described by the equation

$$x=x_0+y\beta\cos\theta+z\beta\sin\theta=g(y,z) \tag{15}$$

Since the conormal vector $\bar{\nu}$ lies in the surface S_M, and since $\varphi=0$ on S_M, the contribution of this surface in Eq. (14) is zero. On $S_w, n_x=n_y=0$, $k=1$, and the conormal coincides with the normal vector. In the case of a lifting wing without thickness, $\partial\varphi/\partial z$ is symmetrical with respect to the plane $z=0$, and the contribution of S_w in the expression (14) is zero. Both surfaces S_g and S_F possess the characteristic direction; hence, $k=1/\beta$ and what remains of Eq. (14) is

$$\int_{S_F}\int\left\{\beta^2\frac{\partial\varphi}{\partial x}+f_y\frac{\partial\varphi}{\partial y}+f_z\frac{\partial\varphi}{\partial z}\right\}dS_F+\int_{S_g}\int\left\{\beta^2\frac{\partial\varphi}{\partial x}+\beta\cos\theta\frac{\partial\varphi}{\partial y}+\beta\sin\theta\frac{\partial\varphi}{\partial z}\right\}dS_g=0 \tag{16}$$

Writing the disturbance velocity potential $\varphi(x,y,z)$ on the surfaces S_F and S_g in the form

$$[\varphi(x,y,z)]_{S_F}=\varphi(x=f(y,z),y,z)=\Phi_F(y,z) \tag{17}$$

respectively,

$$[\varphi(x,y,z)]_{S_g}=\varphi(x=g(y,z),y,z)=\Phi_g(y,z) \tag{18}$$

the integrals over the surfaces S_F and S_g may be transformed into integrals over the projections of the surfaces S_F and S_g on a plane perpendicular to the x axis indicated by S_F^* and S_g^*, respectively,

$$\int_{S_F^*}\int\left\{f_y\frac{\partial}{\partial y}\Phi_F+f_z\frac{\partial}{\partial z}\Phi_F\right\}dydz+\int_{S_g^*}\int\left\{\beta\cos\theta\frac{\partial}{\partial y}\Phi_g+\beta\sin\theta\frac{\partial}{\partial z}\Phi_g\right\}dydz=0 \tag{19}$$

Since for optimum wings $\Phi_F(y,z)$ satisfies Laplace's equation, both integrals in Eq. (19) may be rewritten by means of the divergence theorem

$$\int_{C_{S_F}^*} f\frac{\partial\Phi_F}{\partial n}dC+\beta\int_{C_{S_g}^*}\Phi_g(\cos\theta n_y+\sin\theta n_z)dC=0, \tag{20}$$

where the boundary $C_{S_F}^*$ consists of the projection (Fig. 10) on a plane $x=$ const of the intersection curve of the surface S_F with the Mach cone S_M, with the plane S_g and with the wing S_w. The boundary $C_{S_p}^*$ consists of the projection on a plane $x=$ const of the intersection curve of the plane S_g with the Mach cone S_M, with the wing S_w and with the surface S_F. The intersection curves are called D_0, D_1, and D_2 and are given by

$$D_0\begin{cases}x=\beta\sqrt{y^2+z^2}\\ x=x_0+y\beta\cos\theta+z\beta\sin\theta\end{cases}\rightarrow\begin{cases}z=z_0(y,x_0,\theta)\\ y=y_0(z,x_0,\theta)\end{cases}$$

$$D_1\begin{cases}x=f(y,z)\\ x=x_0+y\beta\cos\theta+z\beta\sin\theta\end{cases}\rightarrow\begin{cases}z=z_1(y,x_0,\theta)\\ y=y_1(z,x_0,\theta)\end{cases}$$

$$D_2\begin{cases}x=f(y,z)\\ x=\beta\sqrt{y^2+z^2}\end{cases}\rightarrow\begin{cases}z=z_2(y)\\ y=y_2(z)\end{cases}$$

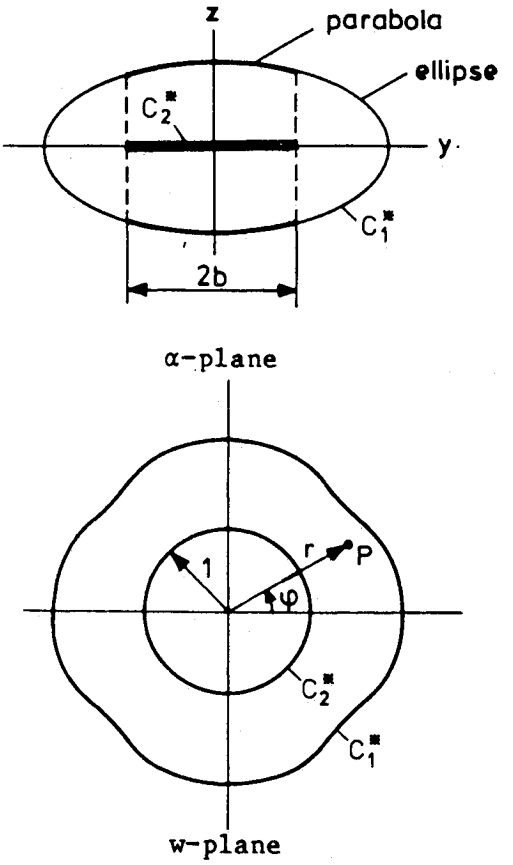

Fig. 6 Control surface in projected and transformed plane.

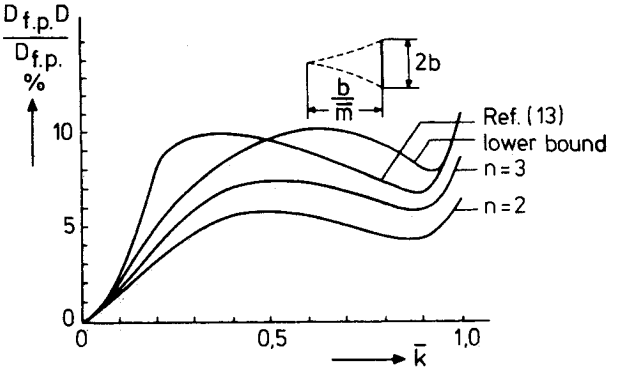

Fig. 7 Variation of drag reduction with slenderness for a delta-like wing.

The boundaries $C_{S_F}^*$ and $C_{S_g}^*$ and, hence, the integration interval in Eq. (20) depend on the parameters x_0 and θ of the plane S_g. Upon differentiation of Eq. (20) with respect to x_0, some manipulation of the result and rearrangement of terms (cf. Ref. 14), one finds the cross-load distribution for an optimum wing expressed as an integral along the intersection curve D_1,

$$\ell(x_0,\theta)=\rho_0U_0\int_C^D\frac{\partial}{\partial x}\Delta\varphi dy=\frac{\rho_0U_0}{\beta\sin\theta}\int_{E^*}^{F^*}\frac{\partial\Phi_F}{\partial n}dC \tag{21}$$
$$(D_1)$$

Since $\Phi_F(y,z)$ satisfies Laplace's equation in S_F^*, Eq. (21) may be rewritten

$$\ell(x_0,\theta)=-\frac{\rho_0U_0}{\beta\sin\theta}\int_{E^*}^{F^*}\frac{\partial\Phi_F}{\partial n}dC \tag{22}$$
$$(D_2)$$

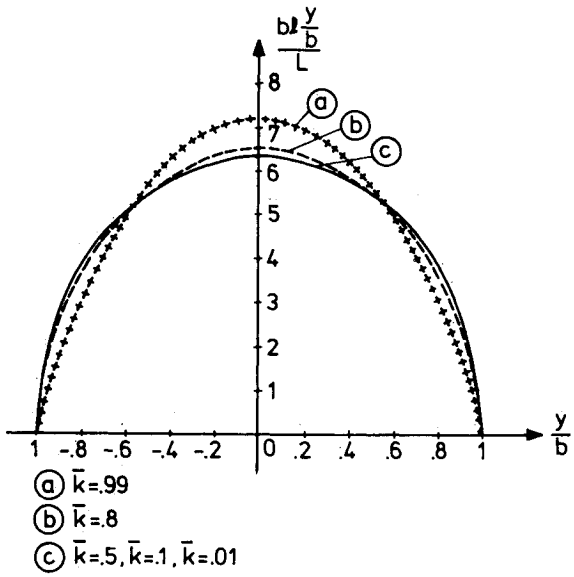

Fig. 8 Influence of slenderness on the optimum spanwise lift distribution for a delta-like wing.

Since Eq. (22) only applies to the optimum wing, $\Phi_F(y,z)$ satisfying Laplace's equation in S_F^*, the expression (22) is quite different from the result obtained by Heaslet and Fuller.[11]

The expression (22) shows that, in order to calculate the optimum cross-load distribution on the wing, it is not necessary to determine the complete distribution of φ on the surface S_F. It is sufficient to calculate $\partial\Phi_F/\partial n$ and Φ_F on the boundaries of S_F^*: C_1^* and C_2^*.

Sonic Trailing Edge

Equation (22) may be applied to the results obtained for a wing with sonic trailing edges [Eqs. (8, 9)], yielding the optimum cross-load distributions

$$\ell(x_0,\theta)=\frac{\pi L}{2c\sin\theta}$$

$$\times 1\Big/\left[\left(\frac{\pi}{2}\right)^2-\left\{E\left(\frac{f}{a}\right)\right\}^2-\frac{a^2-f^2}{f^2}\left\{K\left(\frac{f}{a}\right)-E\left(\frac{f}{a}\right)\right\}^2\right]$$

$$\times\left[\frac{2}{\pi}\left\{K\left(\frac{f}{a}\right)E\left(\psi,\frac{f}{a}\right)-E\left(\frac{f}{a}\right)F\left(\psi,\frac{f}{a}\right)\right\}\cos\psi\right.$$

$$\left.-\frac{2}{\pi}K\left(\frac{f}{a}\right)\sin\psi\sqrt{1-\left(\frac{f}{a}\right)^2\sin^2\psi}\right.$$

$$\left.+\sin\psi\right]_{\psi=-\arcsin\left(\frac{x_0}{c/2}-1\right)-\theta}^{\psi=\arcsin\left(\frac{x_0}{c/2}-1\right)+\pi-\theta} \qquad (23)$$

In Fig. 11 one of the cross-load distributions, the chordwise load distribution, is plotted for various values of $\bar{k}$ [cf. Eq. (10)].

Straight Trailing Edge

The optimum cross-load distributions for a wing with a straight trailing edge are calculated analogously. In Fig. 12 the optimum chordwise load distribution for a wing with a straight trailing edge perpendicular to the oncoming flow is shown for various values of $\bar{k}$.

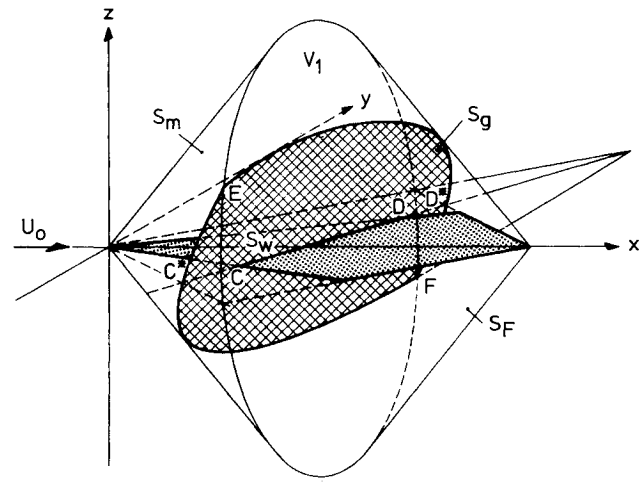

Fig. 9 Region of application of Gauss' divergence theorem.

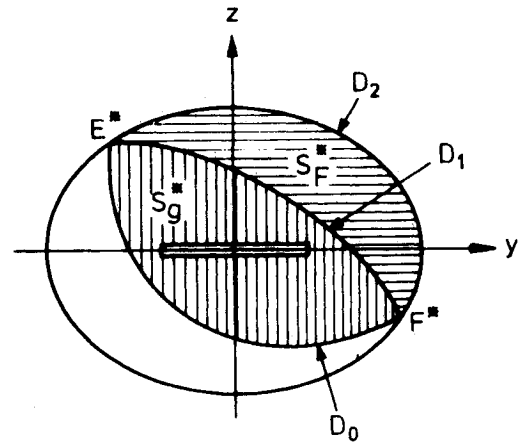

Fig. 10 Projection on a plane $x=$ const of the intersection curves D_0, D_1, and D_2.

Discussion

First, it is observed from Figs. 5 and 8 and from Figs. 11 and 12 that, for planforms considered in the limit as $\bar{k}$ approaches zero, the optimum lift distributions are elliptical. Hence, in general, minimum total drag does not imply minimum vortex drag or minimum wave drag. Second, with respect to the lengthwise distribution of lift, it is observed that, in the neighborhood of the apex of the wing, all distributions are similar and the behavior is dominated by the square root of the distance to the apex. Next, a few remarks are made on the reconstruction of the pressure distribution on the wing from the cross-load distributions for planforms with subsonic leading edges. The reconstruction of the pressure distribution from the cross-load distributions is equivalent to "image reconstruction from projections," which since the middle of this century has been the subject of numerous papers in radioastronomy, electronmicroscopy, and especially radiology (cf. Refs. 15-18). It is known from the literature (cf. Refs. 19 and 20) that the reconstruction of an image is unique only if a complete knowledge of the projections in all directions can be obtained. Since in most of the practical applications only a finite number of projections are given, the information necessary to obtain a reconstruction is supplied by means of interpolation and extrapolation, and a continuous function is fitted as smoothly as possible through the available projections.

In the case of optimized supersonic wings, it is observed from Eq. (15) that the cross-load distributions are known only in directions varying over a finite interval between the two characteristic directions. In addition to these cross-load distributions for optimized supersonic wings, only one

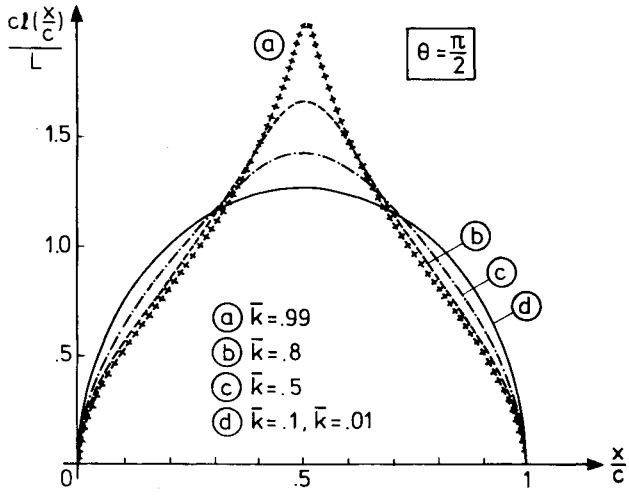

Fig. 11 Influence of slenderness on the optimum chordwise lift distribution for a wing planform with sonic trailing edge.

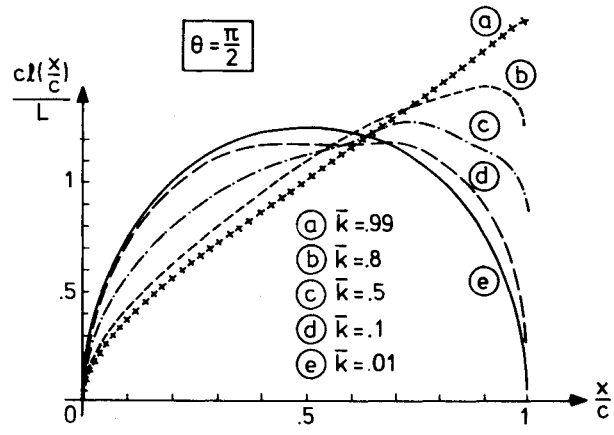

Fig. 12 Influence of slenderness on the optimum chordwise lift distribution for a delta-like wing.

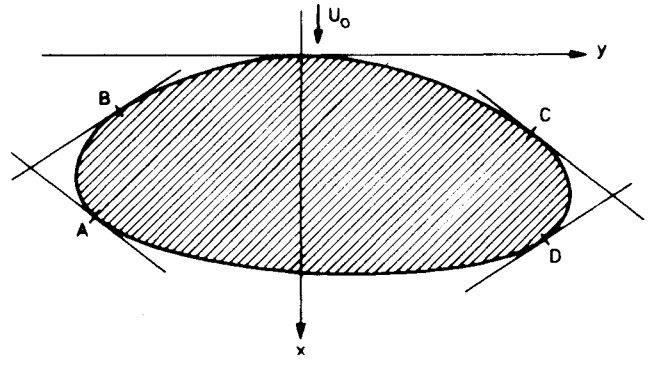

Fig. 13 Example of a planform with continuously curved edges.

isolated distribution is known, the spanwise lift distribution. In this case, one method to supply a complete set of cross loads in an analytic continuation of the cross-load distribution for values of the direction parameter $\beta \cos\theta$ outside the finite interval. Obviously, one of the conditions to be satisfied for application of this extrapolation method is that the analytic continuation of the cross-load distribution converges to the spanwise lift distribution. It is also seen that, for fixed $\beta \cos\theta$, the cross load $\ell(x_0,\theta)$ as a function of x_0 is zero for values of x_0 located outside the interval determined by the projection of the planform edges in the direction $\beta \cos\theta$. Hence, a further condition for the analytic continuation of the cross-load distribution is that the edges of the planform also are continued analytically since they determine the boundaries where $\ell(x_0,\theta)=0$.

Since the segments of the planform edges that determine the boundaries of the cross load when $\beta \cos\theta$ varies over the interval $-\beta \le \beta\cos \le \beta$ also determine the enveloping characteristic surfaces, these parts, in general, form the so-called supersonic parts of these edges (the parts BC and DA in Fig. 13). The latter condition for the application of the method of analytical continuation is a condition on the shape of the planform.

Rephrased, this condition implies that the method of analytical continuation of the optimum cross-load distribution can be applied only if the subsonic parts of the edge of the planform represent an analytical continuation or extrapolation of the supersonic parts. Conversely, if a limited knowledge of the planform exists—for instance, if only the supersonic parts BC and AD in Fig. 13 are known—then a reconstruction by means of an analytical continuation always supplies a pressure distribution on a planform that has smoothly continued edges in the extrapolated area, the parts AB and DC in Fig. 13.

On the other hand, in some optimization cases, for instance, if a planform with subsonic leading edges is considered from a priori knowledge of the planform, one may conclude that the edges contain one or more discontinuities in the curvature. These discontinuities in the curvature result in discontinuities in one of the derivatives of the cross-load distribution with respect to the direction parameter $\beta \cos\theta$. In particular, if it is known that the discontinuities are situated in the extrapolated area, which will be the case for planforms with subsonic leading edges, the method of reconstruction by analytical continuation fails and a different approach has to be chosen.

If the method of extrapolation fails and the cross-load distribution cannot be completed, unique reconstruction cannot be obtained. However, a reconstruction may still be obtained by approximation. In this case, instead of reconstructing the pressure distribution by means of some kind of integral transform, a so-called algebraic reconstruction technique may be applied. For supersonic wings with subsonic leadings edges, this implies that the leading edges passing through the endpoints of the fixed supersonic trailing edge are chosen, and then a sum of known lift distributions on this planform is fitted as accurately as possible in the optimum cross-load distribution.

Thus, the discussion has shown that, since the optimum cross-load distribution is known on the finite interval of the direction parameter $-\beta \le \beta\cos\theta \le \beta$ and for the isolated case $\beta \cos\theta = \pm\infty$, the optimum cross-load distribution contains little information about the subsonic parts of the edges of the planform. In fact, only the spanwise lift distribution ($\beta \cos\theta = \pm\infty$) fixes the maximum span. In particular, for a wing with subsonic leading edges, this implies that a class of leading edges and corresponding pressure distributions seems to fit in the optimum cross-load distribution.

Concluding Remarks

The planform optimization for nonslender supersonic delta-like wings with subsonic leading edges has been studied. Based on momentum flux theory, a method has been outlined to find the optimum spanwise lift distribution and the optimum cross-load distributions producing a given lift at minimum drag. These distributions depend on the supersonic parts of the planform edges only. For delta-like wings with subsonic leading edges, this implies that only the form of the trailing edge determines the optimum distributions. The method has been applied to delta-like wings with two types of the trailing edges. First, the results indicate that, depending on the slenderness of the planform, introduction of the proper camber and twist or leading-edge

curvature yields a gain in drag up to 10% with respect to an uncambered flat plate wing with straight leading edges. Second, no optimum form of subsonic leading edge exists. For a given trailing edge, a different camber and twist distribution corresponds to each curved subsonic leading edge, producing the optimum cross-load distributions.

Acknowledgments

The author wishes to acknowledge the interest and support of Prof. J.A. Steketee for the research contained in this paper.

References

[1]Cohen, D., "The Warping of Triangular Wings for Minimum Drag at Supersonic Speeds," *Journal of the Aeronautical Sciences,* Vol. 24, Jan. 1957, pp. 67-68.

[2]Tsien, S. H., "The Supersonic Conical Wing of Minimum Drag," *Journal of the Aeronautical Sciences,* Vol. 22, Dec. 1955, pp. 805-817.

[3]Fenain, M. and Valléé, D., "Application de la théorie des écoulements homogénes á la recherche de l'adaption de certaines ailes en régime supersonique," Onéra Mémo Technique 14, 1958.

[4]Jones, R. T., "The Minimum Drag of Thin Wings in Frictionless Flow," *Journal of the Aeronautical Sciences,* Vol. 18, Feb. 1951, pp. 75-81.

[5]Jones, R. T., "The Theoretical Determination of the Minimum Drag of Airfoils at Supersonic Speeds," *Journal of the Aeronautical Sciences,* Vol. 19, Dec. 1952, pp. 813-822.

[6]Jones, R. T., "Reduction of Wave Drag by Antisymmetric Arrangements of Wings and Bodies," *AIAA Journal,* Vol. 10, Feb. 1972, pp. 171-176.

[7]Jones, R. T., "Some Observations on Supersonic Wing Design," *Proceedings of Evolution of Aircraft Wing Design Symposium,* Air Force Museum, Dayton, Ohio, March 1980, pp. 91-94.

[8]Ward, G. N., "On the Minimum Drag of Thin Lifting Bodies in Steady Supersonic Flows," Aeronautical Research Council fm 2459, Oct. 1956.

[9]Kogan, M. N., "On Bodies of Minimum Drag in a Supersonic Gas Stream," *Prikladnaya Matematika i Mekhanika,* Vol. XXI, No. 2, 1957, pp. 207-212.

[10]Zhilin, Yu.L., "Minimum Drag Wings," *Prikladnaya Matematika i Mekhanika,* Vol. XXI, No. 2, 1957, pp. 213-220.

[11]Heaslet, M. A. and Fuller, F. B., "Drag Minimization for Wings in Supersonic Flow with Various Constraints," NACA TN 4227, Feb. 1958.

[12]Bos, H. J., "The Lifting Wing with Minimum Drag in Supersonic Flow," University of Technology, Delft, the Netherlands, Rept. LR-234, Aug. 1977.

[13]Germain, P. and Gibault, R., "Quelques résultats sur les ailes delta portantes a trainée minimum en régime supersonique," *La Récherche Aéronautique,* Vol. 63, April 1958, p. 39.

[14]Bos, H. J., "On the Aerodynamic Optimization of Supersonic Wings," Thesis, University of Technology, Delft, the Netherlands, Feb. 1984.

[15]Bracewell, R. N., "Strip Integration in Radio Astronomy," *Australian Journal of Physics,* Vol. 9, 1956, pp. 198-217.

[16]Cormack, A. M., "Representation of a Function by Its Line Integrals, with Some Radiological Applications II," *Journal of Applied Physics,* Vol. 35, No. 10, Oct. 1964, pp. 2908-2913.

[17]Helgason, S., "The Radon Transform," *Progress in Mathematics,* Birkhäuser, Boston, MA, 1980.

[18]Lewitt, R. M. and Bates, R. H. T. "Image Reconstruction from Projections I-IV," *Optik,* Vol. 50, 1978, pp. 19-33, 85-109, 189-204, 269-278.

[19]Herman, G. T. (ed.), *Image Reconstruction from Projections: The Fundamentals of Computerized Tomography,* Academic Press, New York, 1980.

[20]Smith, K. T., Solomon, D. C., and Wagner, S. L., "Practical and Mathematical Aspects of the Reconstruction of Objects from Radiographs," *Bulletin of the American Mathematical Society,* Vol. 83, No. 6, Nov. 1977, pp. 1227-1270.